Neutron-Activation Cross Sections*

J. A. MISKEL, K. V. MARSH, M. LINDNER, AND R. J. NAGLE
Lawrence Radiation Laboratory, University of California, Livermore, California
(Received March 23, 1962)

Neutron-activation cross sections have been measured for five target nuclei, Hf^{180}, Ta^{181}, W^{186}, Au^{197}, and Th^{232}, over a neutron energy range from 0.030 to 4.0 MeV. The experimental results are compared with values calculated from the statistical theory of nuclear reactions. Values of the constant C_n in the approximate level density formula $p_n = C_n \exp[2(aE)^{1/2}]$ are obtained for these isotopes from a fit of the calculated and measured cross sections above 1 MeV.

INTRODUCTION

THE energy dependence and absolute values of neutron-capture cross sections are of interest for nuclear reaction[1–4] and element-formation[5] theories. Three techniques for measuring capture cross sections are in common use: spherical shell transmission measurements,[6–8] capture gamma-ray measurements[9,10] and activation measurements.[11,12] Comparisons of the three techniques are given below.

Spherical shell transmission measurements do not depend on absolute detection efficiencies and therefore can give quite accurate capture cross sections; but they require the use of large samples, and the corrections for self-shielding effects are sometimes difficult to evaluate. Capture gamma-ray measurements also result in accurate capture cross-section measurements when the efficiencies of the gamma-ray detector are known for the prompt radiations involved; but, at energies above the threshold for it, the $(n,n'\gamma)$ reaction cannot be distinguished from the (n,γ) reaction. Both the transmission and capture gamma techniques require separated isotopes if specific reactions are to be measured.

The activation technique measures the cross section for formation of a specific product and has high sensitivity; it is limited, however, to product nuclides with a convenient half-life.

In this work, measurements have been made of the activation cross sections of five target nuclei, Hf^{180}, Ta^{181}, W^{186}, Au^{197}, and Th^{232}, over a neutron energy range from 0.030 to 4.0 MeV. The radioactivities produced in the target nuclei by neutron capture have been used to determine the activation cross sections.

The experimental results are compared with values calculated from the statistical theory of nuclear reactions. For neutron energies less than 1 MeV, the treatment of Margolis[1] was used; for neutron energies greater than 1 MeV, another treatment suggested by Margolis[13] was used.

EXPERIMENTAL

Bombardments

Neutrons of known energy were produced by either the $Li(p,n)$ reaction or the $T(p,n)$ reaction. Monoenergetic protons were obtained from one of several Van de Graaff generators. The source of protons, target reaction, and neutron energy for each bombardment are given in Table I.

The materials to be activated were prepared in the form of 1.007-in.-diam disks cut from 0.005- or 0.010-in. sheet. Packets were prepared by wrapping the stacked foils in thin (0.0005-in.) aluminum foil. These packets were then encased in 0.015-in. cadmium sheet to minimize activation by neutrons scattered below the cadmium cutoff. (In run LA-1, no cadmium was used since a previous measurement[14] had shown that only negligible activation was produced by the neutrons scattered into this energy region under the conditions of the experiment.) The target packets were placed on the circumference of a circle of 10-cm radius; the center of the circle was at the center of the proton target. The angle subtended by the target packets at the source was approximately 15°.

The neutron flux incident on the target packet was determined, for each irradiation with the $T(p,n)He^3$ source, by monitoring the flux, at a known angle, with a fission counter and using the angular distribution versus intensity data.[15–17] In the experiment in which the neu-

* Work done under the auspices of the U. S. Atomic Energy Commission.
[1] B. Margolis, Phys. Rev. **88**, 327 (1952).
[2] H. Feshbach, C. Porter, and V. F. Weisskopf, Phys. Rev. **96**, 448 (1954).
[3] A. M. Lane and J. E. Lynn, Proc. Phys. Soc. (London) **A70**, 557 (1957).
[4] C. Mossin-Kotin, B. Margolis, and E. S. Troubetzkoy, Phys. Rev. **116**, 937 (1959).
[5] E. M. Burbidge, G. R. Burbidge, W. A. Fowler, and F. Hoyle, Revs. Modern Phys. **29**, 547 (1957).
[6] A. O. Hansen, Los Alamos Scientific Laboratory Rept. LA-276, 1945 (unpublished).
[7] H. Bethe, J. R. Beyster, and R. Carter, J. Nuclear Energy **3**, 207, 273 (1956); **4**, 3, 147 (1957).
[8] H. W. Schmitt and C. W. Cook, Nuclear Phys. **20**, 202 (1960).
[9] C. Diven, J. Terrell, and A. Hemmendinger, Phys. Rev. **120**, 556 (1960).
[10] J. H. Gibbons, R. L. Macklin, P. D. Miller, and J. H. Neiler, Phys. Rev. **122**, 182 (1961).
[11] E. Segrè, K. Greisen, G. A. Linenberger, and J. A. Miskel, Atomic Energy Commission Report MDDC-228, 1946 (unpublished).
[12] A. E. Johnsrud, M. G. Silbert, and H. H. Barschall, Phys. Rev. **116**, 927 (1959).
[13] B. Margolis (private communication, 1961).
[14] A. Schardt (private communication, 1958).
[15] N. Jarmie and J. D. Seagrave, Los Alamos Scientific Laboratory Report LA-2014 1957 (unpublished).
[16] J. Perry, Los Alamos Scientific Laboratory (private communication).
[17] J. L. Fowler and J. E. Brolley, Jr., Revs. Modern Phys. **28**, 103 (1956).

TABLE I. Neutron-activation cross sections.

Run[a]	Neutron source	E_p (MeV)	Target thickness (MeV)	Target length[b] (cm)	Angle (deg)	E_n (MeV)	$\sigma(n,\gamma)$ (mb) Hf^{180}	Ta^{181}	W^{186}	Au^{197}	Th^{232}
LA-5	Li(p,n)	2.032	0.038	···	127.5	0.032±0.009	228	1073	281	947	819
					112.5	0.042±0.011	195	940	249	838	615
					97.5	0.059±0.013	194	431	258	833	409
BNL-1	T(p,n)	1.617	0.034	···	160	0.069±0.004		654	289	629	363
LA-5	Li(p,n)	2.032	0.038	···	82.5	0.084±0.016	147	501	194	530	350
					67.5	0.118±0.018	112	427	150	409	306
BNL-3	T(p,n)	1.850	0.087	···	160	0.112±0.011		356	158	401	217
LA-5	Li(p,n)	2.032	0.038	···	45	0.176±0.021	187	313	98	378	204
LA-1	T(p,n)	1.888	0.173	3.0	105	0.240±0.04		324	104	353	177
LA-5	Li(p,n)	2.032	0.038	···	0	0.247±0.024		282	85	367	219
BNL-2	T(p,n)	2.440	0.074	···	160	0.255±0.01		215	81	274	141
LA-4	T(p,n)	3.07	0.17	3.2	135.5	0.430±0.023	42.0	167	86	208	148
LA-1	T(p,n)	1.888	0.173	3.0	60	0.580±0.07		188	71	180	153
LA-3	T(p,n)	4.00	0.08	3.1	137.4	0.710±0.015	38.5	110	53.3	113	145
BNL-1	T(p,n)	1.617	0.034	···	0	0.79 ±0.021		184	74	150	157
LA-2	T(p,n)	4.811	0.140	3.1	153.3	0.85 ±0.02	46.5	87	44	91.6	112
LA-1	T(p,n)	1.888	0.173	3	30	0.87 ±0.08		140	65	123	148
BNL-3	T(p,n)	1.850	0.087	···	0	0.99 ±0.05		124	62	128	133
LA-1	T(p,n)	1.888	0.173	3	0	1.00 ±0.09		127	58	108	138
BNL-2	T(p,n)	2.440	0.074	···	0	1.61 ±0.04		83	44	94.3	99.7
LA-4	T(p,n)	3.07	0.17	3.2	30	1.79 ±0.08	39.1	65	37	78	84
LA-4	T(p,n)	3.07	0.17	3.2	0	2.00 ±0.09	32	55.5	31	64	61
LA-3	T(p,n)	4.041	0.08	3.1	30	2.72 ±0.04	25	29	21	34	28
	T(p,n)	4.041	0.08	3.1	0	3.00 ±0.04	23	24	16	29.5	23.1
LA-2	T(p,n)	4.811	0.140	3.1	28	3.65 ±0.07	16.7	15.8	10.1	21.1	15.1
	T(p,n)	4.811	0.140	3.1	0	3.97 ±0.07	16.4	14.1	9.0	19.4	13.5

[a] Runs numbered BNL-1, 2, and 3 were made with the Brookhaven Van de Graaff generator; LA-1 and 5 with the Los Alamos low-energy Van de Graaff generator; LA-2, 3, and 4 with the Los Alamos high-energy Van de Graaff generator.
[b] Reported only for gas targets.

trons were produced by the Li(p,n) reaction, the neutron flux was determined at each angle at which target foils were placed with a fission counter. The U^{235} fission cross sections reported by Allen and Henkel[18] were used to calculate the neutron fluxes from the observed fissions.

ACTIVATION MEASUREMENT

With the exception of Th^{233}, the activations produced were determined by gamma-ray counting of the irradiated foils with NaI(Tl) scintillation counters. The gamma counters were calibrated for each isotope by measurement of the count rate of a thin (weightless) sample whose beta-ray disintegration rate had previously been determined in a 4π proportional counter. Self-absorption and scattering in the foils and scattering from the materials associated with the counters were experimentally determined. The observed count rates were thus directly convertible to disintegration rates.

The Th^{233} produced by irradiation of the Th^{232} foil was determined by measurement of its 27.4-day daughter, Pa^{233}. The thorium foil was dissolved, Pa^{231} tracer added, the protactinium chemically isolated. The Pa^{233} β rays were counted with an end-window, methane-flow, proportional counter. As with the scintillation counters, the counting efficiency of this counter for Pa^{233} radiations was determined by comparison with the 4π counter.

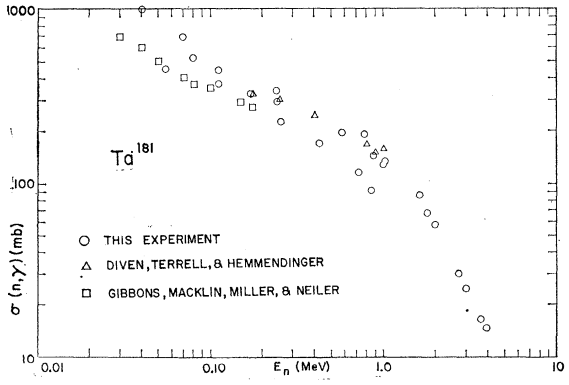

FIG. 1. Experimental results for Ta^{181}. Representative data published by other experimenters are shown for comparison.

RESULTS

The observed activities were converted to disintegration rates, extrapolated in time to the end of irradiation, and corrected for decay during bombardment. The activation cross sections calculated from these data and the neutron fluxes are listed in Table I and presented graphically in Figs. 1–5. Representative data obtained by other investigators are included on these graphs for the purpose of comparison.

The uncertainty in neutron energy for a given run arises from the following sources: (1) the spread in incident proton energy; (2) the finite target thickness; and (3) the finite extension of the source (in those bom-

[18] R. L. Henkel, Los Alamos Scientific Laboratory Report LA-2114, 1957 (unpublished).

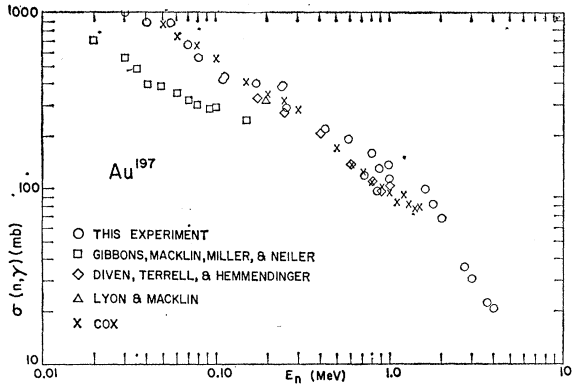

FIG. 2. Experimental results for Au^{197}. Representative data published by other experimenters are shown for comparison.

bardments employing a gaseous tritium target). The contributions of these sources to the uncertainty in the neutron energy vary with the target used, the proton energy, and the angle at which the foil packets were placed. These factors were evaluated to obtain the errors quoted for each neutron energy in Table I. The quoted errors do not include the uncertainty in the fission cross sections used to determine the fluxes or, in the case of the $T(p,n)$ reaction, in the angular distribution vs intensity data.

Uncertainties in the values of the cross sections determined from these activation measurements can arise from several sources. These are (1) the finite angular width of the targets, (2) the determination of the number of reactions that occurred, and (3) absorption and scattering of the neutrons in the target packets. The contributions of each of these factors to the uncertainty in the measured cross sections are discussed below.

The error resulting from the finite width of the target foils is less than 2%. For targets placed at angles other than 0° with respect to the neutron beam, the variations in cross section and intensity with energy are such that the average cross section observed represents the cross section calculated for the neutron energy incident on the center of target foil to less than 1%.

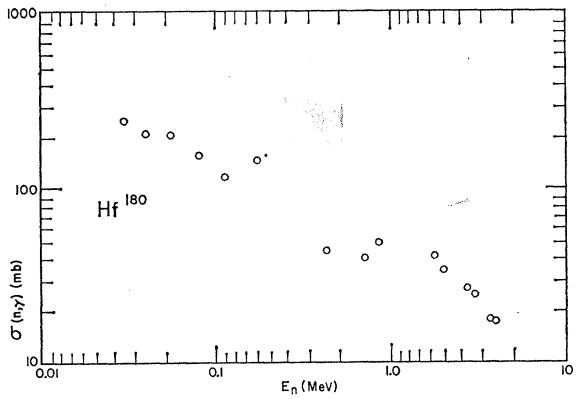

FIG. 3. Experimental results for Hf^{180}.

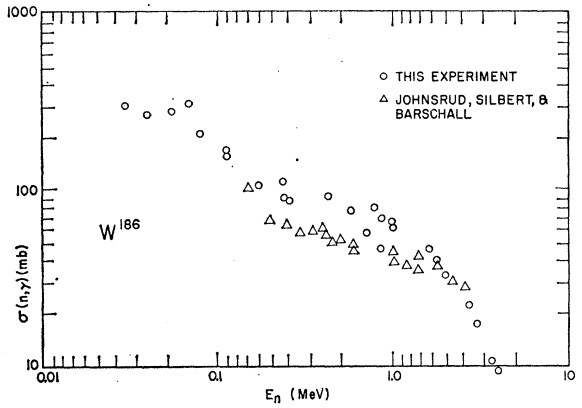

FIG. 4. Experimental results for W^{186}. Representative data published by other experimenters are shown for comparison.

For foils placed at 0°, the uncertainty is less than 2% because of the relatively small variation in energy over the angle subtended by the target.

The error in the determination of the number of reactions that occurred in the target foil depends upon the accuracy of the calibration of the counters and the statistics of the measurements of the decay rates of the samples. The calibrations of the counters against the 4π counter, and the efficiency of the 4π counter produce an error of no more than 3% in the final result. With the exception of the hafnium and tantalum samples, which were of extremely low count rate, the statistical accuracy of the activity, extrapolated to the end of irradiation, is better than 1%. The hafnium and tantalum extrapolated activity values are uncertain by less than 4%.

The total thickness of the foil packets was about 0.12 cm, and the average density of nuclei in each packet was $\sim 5\times 10^{22}$ nuclei/cm^3. The attenuation of the neutron beam by absorption was, therefore, negligible. The error arising from the scattering of neutrons in the target packet can be calculated by the method of Schmitt.[19]

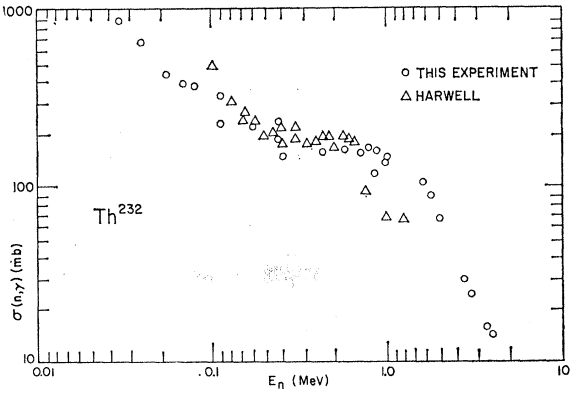

FIG. 5. Experimental results for Th^{232}. Representative data published by other experimenters are shown for comparison.

[19] H. W. Schmitt, Oak Ridge National Laboratory Report ORNL-2883 (unpublished).

Under our experimental conditions, the error in the cross sections resulting from neutron scattering in the target depends upon the position of the particular foil in the packet. The cross section measured for the foil first seen by the neutrons is approximately 2% higher than the true value, and that for the last foil seen by the neutrons is approximately 8% higher. Since the relative positions of the foils during the various irradiations was not recorded, the values of the cross sections measured directly are at least 2% too high and may be as much as 8% too high.

The cross-section values listed in Table I have been corrected for the self-scattering effect by decreasing the observed values by 5%, and adding an uncertainty of ±3%. Thus, the maximum error in the cross sections arising from the sources discussed above, should be about ±10%.

The results for Au^{197} are in good agreement with those of Cox,[20] Lyon, and Macklin,[21] Macklin *et al.*,[22] and Diven *et al.*[9] There is, however, considerable disagreement between our results and those of Gibbons *et al.*,[10] both in magnitude and in energy dependence.

The results for Ta^{181} are in fair agreement with those of Diven *et al.*[9] between 0.25 and 1.0 MeV, but are in poor agreement with those of Gibbons *et al.*[10] below 0.15 MeV.

The data for Th^{232} are in substantial agreement with the other reported results below 0.7 MeV, but they disagree with the Harwell results above 0.7 MeV. The data for W^{186} are in poor agreement with those of Johnsrud *et al.*[12] There are no published data for comparison with the Hf^{180} results.

DISCUSSION

The activation cross section, $\sigma_E(n,\gamma)$, for neutrons of energy E is given by

$$\sigma_E(n,\gamma)=\sigma_C\Gamma_\gamma/\Gamma, \tag{1}$$

where σ_C is the cross section for formation of the compound nucleus, Γ_γ is the radiation width, and Γ is the total width.

Following the treatment of Margolis,[1] one can write the capture cross section as

$$\sigma_E(n,\gamma)=\frac{\pi\lambda^2}{2(2i+1)}\sum_{l=0}^{\infty}T_l(E) \times\sum_{J=0}^{\infty}\frac{\epsilon_{jl}{}^J(2J+1)}{1+\xi_J f_{\Delta I}(E)\Sigma_{l'}\Sigma_n\epsilon_{jnl'}{}^J T_{l'}(E-E_n)}, \tag{2}$$

where i is the spin of the target nucleus, j is the channel spin, λ is the wavelength of the incident neutron, T_l is the transmission coefficient for the lth partial wave,

[20] S. A. Cox, Phys. Rev. **122**, 1280 (1961).
[21] W. S. Lyon and R. L. Macklin, Phys. Rev. **114**, 1619 (1959).
[22] R. L. Macklin, N. H. Lazar, and W. S. Lyon, Phys. Rev. **107**, 504 (1957).

TABLE II. Parameters used to calculate capture cross sections below 1 MeV. Separation energies from reference 24.

	Target nucleus					Compound nucleus		
	Ground state		Excited levels				Separation energy	reference
	spin	parity	energy	spin	parity	ξ_J	(MeV)	
$_{72}Hf^{180}$	0	+	93	2	+	196	5.358	25
			309	4	+			
			641	6	+			
			1084	8	+			
			1142	8	−			
$_{74}W^{186}$	0	+	123	2	+	255	5.325	26
			750	2	+			
$_{90}Th^{232}$	0	+	50	2	+	71.2	4.992	27
			163	4	+			
			330	6	+			
			550	8	+			
			725	0	+			
			775	2	+			
			788	2	+			
			820	10	+			
			875	4	+			
			1045	1	−			
			1095	3	−			
$_{73}Ta^{181}$	7/2	+	6.24	9/2	−	12.9	5.643	28, 29
			136	9/2	+			
			158.8	11/2	−			
			301	11/2	+			
			482	5/2	+			
			615	1/2	+			
			619	3/2	+			
$_{79}Au^{197}$	3/2	+	77	1/2	+	20.4	6.000	29
			268	3/2	+			
			279	5/2	+			
			409	11/2	−			
			548	7/2	+			

$\epsilon_{jl}{}^J$ is a statistical factor defined by[23]

$$\epsilon_{jl}{}^J=\left\{\begin{matrix}2,\text{ if both } j_1 \text{ and } j_2 \text{ satisfy}\\ 1,\text{ if } j_1 \text{ or } j_2 \text{ (not both) satisfies}\\ 0,\text{ if neither } j_1 \text{ nor } j_2 \text{ satisfies}\end{matrix}\right\} \times|J-l|\leq j\leq(J+l),$$

J is the spin of a level in the compound nucleus, E_n is the energy of the nth excited state of the target nucleus, and l' is the angular momentum of the emitted neutron. ξ_J is defined as $D_J/2\pi\Gamma_\gamma$, where Γ_γ is the radiation width and D_J the spacing between levels of the same spin and parity, and $f_{\Delta I}(E)$ is given by

$$f_{\Delta I}(E)=\int_0^B\epsilon^{2\Delta I+1}\rho(B-\epsilon)d\epsilon\Big/\int_E^{B+E}\epsilon^{2\Delta I+1}\rho(B+E-\epsilon)d\epsilon, \tag{2a}$$

where B is the neutron binding energy; $\rho(E)$, the level density at excitation E, is given by

$$\rho(E)=C\exp[2(aE)^{1/2}].$$

ϵ and $2^{\Delta I}$ are the energy and multiple order, respectively, of the gamma radiation emitted in the decay of the com-

[23] W. Hauser and H. Feshbach, Phys. Rev. **87**, 366 (1952).

pound nucleus. In the cross-section calculations made, the radiative transitions were assumed to be of dipole origin.

Calculations of the capture cross sections as a function of energy for each of the five nuclides were made from Eq. (2) for neutron energies from 0.01 to 1.0 MeV with the aid of an IBM 650 computer. Partial-wave contributions from $l=0$ to $l=5$ were included. Energy levels in the target nucleus were taken from the published data.[24–29] The values used for each nucleus are shown in Table II.

The effect, on the cross section, of the value of a in the level density formula was examined by calculating the cross sections with both $a=A/10$ and $a=A/20$. Although, for neutron energies below 1 MeV, the effect was in general small, $a=A/20$ appeared to give a better fit to the experimental data than $a=A/10$. In the calculations of the cross section for $E_n>1$ MeV, however, the value $a=A/10$ gave much better agreement with the experimental data.

Three different values of the parameter ξ_J were used to calculate the cross section for each nuclide: (1) the value obtained by use of the experimental low-energy

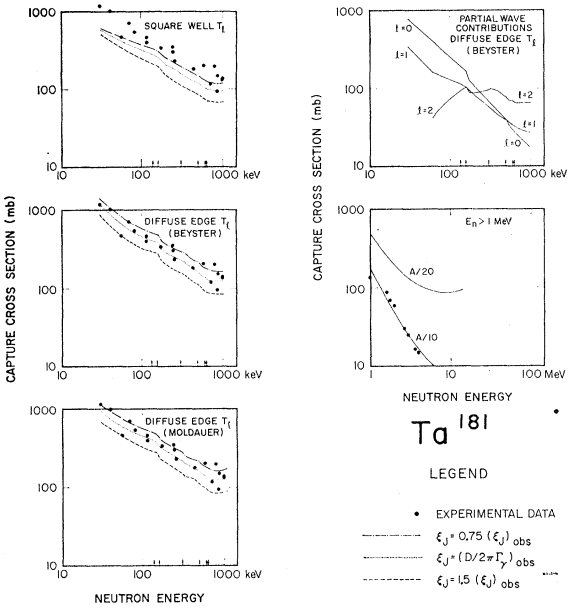

FIG. 6. Comparison of experimental and calculated cross sections for Ta^{181}. The source of the transmission coefficients (T_l) used in the calculations is indicated on each curve. $(\xi_J)_{obs}$ is obtained from reported low-energy resonance data. The arrows indicate positions of known levels in the target nucleus (Table II). The high-energy data ($E_n>1$ MeV) were calculated by Eq. (3) in the text.

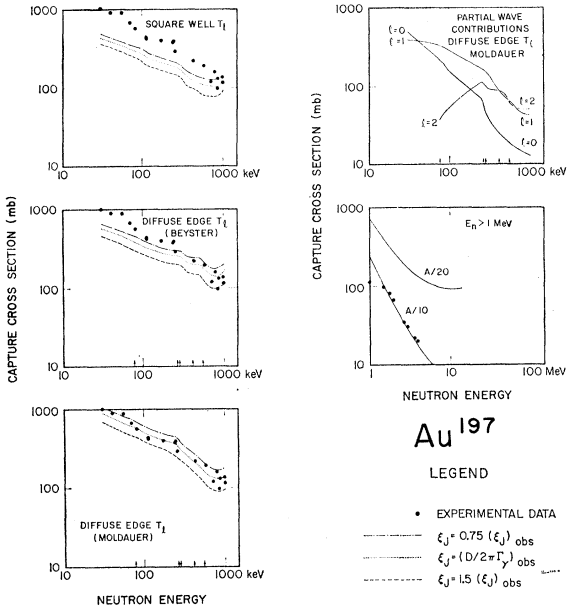

FIG. 7. Comparison of experimental and calculated cross sections for Au^{197}. The source of the transmission coefficients (T_l) used in the calculations is indicated on each curve. $(\xi_J)_{obs}$ is obtained from reported low-energy resonance data. The arrows indicate positions of known levels in the target nucleus (Table II). The high-energy data ($E_n>1$ MeV) were calculated by Eq. (3) in the text.

resonance data[30] for level densities and radiation widths, (2) a value 1.5 times this, and (3) a value 0.75 times this. Three sets of transmission coefficients were used in the calculations. One set was obtained from a complex square well model, according to the treatment of Moore,[31] and the other two sets from a model with a spherical complex well and diffuse edges,

$$V=\frac{-V_0(1+i\xi)}{1+\exp[2(r-r_0)/d]},$$

according to the treatments of Moldauer[32] and Beyster.[33] The Beyster treatment differs from that of Moldauer in that V_0 is varied with energy and a different value is used for the nuclear radius. A table of T_l values as a function of Z, A, and E is given by Beyster in reference 33. The values of T_l for the Moldauer treatment were obtained by interpolation from tables in reference 31.

The results of each set of calculations are compared with the experimental values of the cross sections in Figs. 6–10. In all cases, as can be seen from the figures

[24] A. G. W. Cameron, Chalk River Laboratory Report AECL-433, 1957 (unpublished).
[25] M. Deutsch and R. W. Bauer, Nuclear Phys. **21**, 128 (1960).
[26] A. V. Cohen and J. A. Cookson, Nuclear Phys. **23**, 32 (1961).
[27] B. Elbeck, R. Diamond, and F. Stephens (private communication).
[28] A. H. Muir and F. Boehm, Phys. Rev. **122**, 1564 (1961).
[29] D. Strominger, J. M. Hollander, and G. T. Seaborg, Revs. Modern Phys. **30**, 585 (1958).
[30] *Neutron Cross Sections*, compiled by D. J. Hughes and R. Schwartz, Brookhaven National Laboratory Report BNL-325 (Superintendent of Documents, U. S. Government Printing Office, Washington, D. C. 1958), 2nd ed.
[31] R. G. Moore, Jr., Revs. Modern Phys. **32**, 101 (1960).
[32] P. A. Moldauer, Argonne National Laboratory Report ANL-6323, 1961 (unpublished). The values of T_l reported herein were obtained directly from the values of $\sigma_{C(l)}/\pi R^2$ tabulated by E. J. Campbell, H. Feshbach, C. E. Porter, and V. F. Weisskopf in Atomic Energy Commission Report TID-5820 (unpublished).
[33] J. R. Beyster, Los Alamos Scientific Laboratory Report LA-2099, 1957 (unpublished).

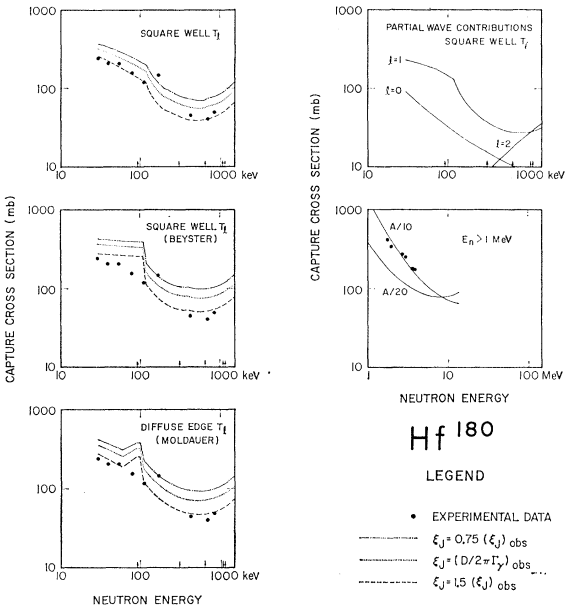

FIG. 8. Comparison of experimental and calculated cross sections for Hf^{180}. The source of the transmission coefficients (T_l) used in the calculations is indicated on each curve. $(\xi_J)_{obs}$ is obtained from reported low-energy resonance data. The arrows indicate positions of known levels in the target nucleus (Table II). The high-energy data ($E_n > 1$ MeV) were calculated by Eq. (3) in the text.

(except for Hf^{180} where the data are scarce), the experimental data are in better agreement with the values calculated using the potential well with diffuse edges than with the values calculated using the square well. It also appears that, except in the case of Th^{232}, values of Γ_γ/D obtained directly from the low-energy resonance data give the best agreement with experiment.

Figures 6–10 also show the partial-wave components of the theoretical curve that gave the best fit to the experimental data. Some of the discontinuities that appear in the calculated cross sections are probably due to the method of calculation. It was necessary to use a finite value (10^{-3}) for the lower limit of the transmission coefficients included in the calculation of a cross section. Thus, the contribution of a given l wave may change abruptly from zero to a finite fraction of the total capture cross section as the value of T_l changes from zero (i.e., less than 10^{-3}) to 10^{-3} or greater. However, sudden changes in the magnitudes of a partial-wave contribution in the vicinity of an excited level in the target nucleus, such as that for the d wave in W^{186}, can be attributed to the availability of a new exit channel for these neutrons and are not due to the calculational limitations described above.

In the energy region above about 1 MeV, the increasing density of levels in the target nucleus makes the calculation of the cross section from Eq. (2) virtually impossible. Therefore, in this energy region a J-independent approximate formulation due to Margolis[13] was used in conjunction with a formula for the level densities to evaluate the cross sections. The cross section is expressed as

$$\sigma_E(n,\gamma)=\frac{\pi\hbar^2\Gamma_\gamma}{mD_c}\int_E^{B+E}\epsilon^3\rho_c(E+B-\epsilon)d\epsilon \Big/ C_n\int_0^E\epsilon_n\rho_n(E-\epsilon_n)d\epsilon_n\int_0^B\epsilon^3\rho_c(B-\epsilon)d\epsilon, \quad (3)$$

where ρ_c and ρ_n, the level densities in the compound nucleus and target nucleus, respectively, are given by

$$\rho_c=C_c\exp\{2[a(B+E-\epsilon)]^{1/2}\},$$
$$\rho_n=C_n\exp\{2[a(E-\epsilon)]^{1/2}\}.$$

E is the excitation energy, a is the level density parameter, and m is the mass of the neutron.

Calculations were made with this formula using values listed in Table III for the parameters. The sources of these values are also given in Table III.

The calculated curves and the experimental points are shown in Figs. 6–10. The energy dependence of the cross section is sensitive to the choice of a; therefore, calculations were made using both $a=A/10$ and $a=A/20$. Only $a=A/10$ gave an energy dependence in good agreement with the experimental values. The values of cross sections for each isotope (except Th^{232}) were adjusted to fit the experimental data by choosing C_n. The value of C_n thus chosen for each isotope is given in column 5 of Table III. The values of C_n given by Blatt and Weisskopf[34] for odd nuclei only are listed in column 6 of the table for comparison.

The value of C_n for Th^{232} cannot be obtained by adjustment of the calculated cross section to fit the experimental data since, above 1.10 MeV, the fission process competes with radiative capture. It was noted that for the even-even nuclei the values of C_n obtained by adjustment of the theoretical cross sections were in substantial agreement with the values obtained by accounting for the pairing energy by applying the rule of Bullock and

TABLE III. Parameters used to calculate capture cross sections above 1 MeV.

Target	B[a]	Γ_γ[b]	D_c[b]	C_n[c]	C_n[d]
Hf^{180}	5.358	0.060	73.9	0.0024	0.01
W^{186}	5.325	0.046	73.7	0.0022	0.01
Th^{232}	4.992	0.035	16.8	0.001	0.005
Au^{197}	6.000	0.125	21.6	0.006	0.007
Ta^{181}	5.643	0.056	4.47	0.0244	0.01

[a] The energy listed is the separation energy of a neutron from the compound nucleus and is obtained from reference 24.
[b] Reference 30.
[c] From best fit of the data.
[d] Reference 34.

[34] J. M. Blatt and V. F. Weisskopf, *Theoretical Nuclear Physics* (John Wiley & Sons, Inc., New York, 1952).

Moore,[35]

$$\tfrac{1}{2}C_{\text{odd-odd}}=C_{\text{odd-}A}=5C_{\text{even-even}},$$

to the values given by Blatt and Weisskopf for odd-A nuclei. The cross section for Th^{232} was calculated using a value for C_n obtained by application of the Bullock and Moore rule to the C_n for $A=231$ given by Blatt and Weisskopf. The calculated cross sections for Th^{232} are somewhat higher than the observed ones, as might be expected since no allowance is made in Eq. (3) for fission competition.

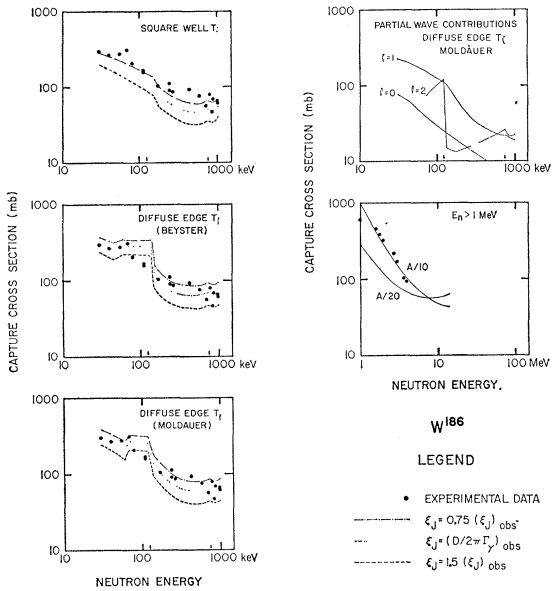

FIG. 9. Comparison of experimental and calculated cross sections for W^{186}. The source of the transmission coefficients (T_l) used in the calculations is indicated on each curve. $(\xi_J)_{\text{obs}}$ is obtained from reported low-energy resonance data. The arrows indicate positions of known levels in the target nucleus (Table II). The high-energy data ($E_n>1$ MeV) were calculated by Eq. (3) in the text.

[35] R. E. Bullock and R. G. Moore, Jr., Phys. Rev. **119**, 721 (1960).

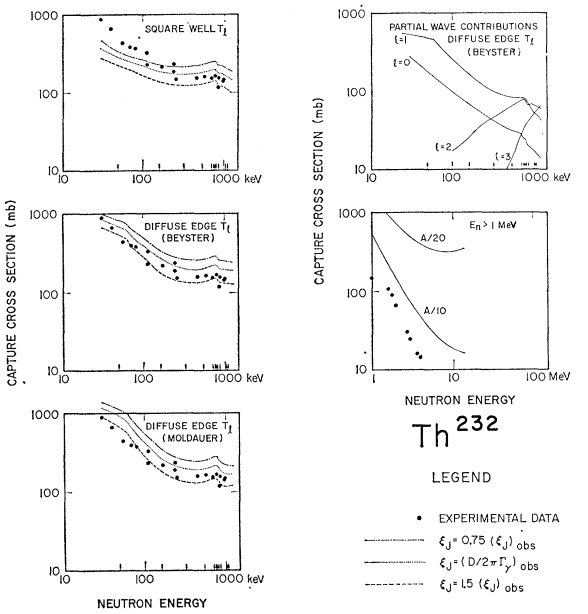

FIG. 10. Comparison of experimental and calculated cross sections for Th^{232}. The source of the transmission coefficients (T_l) used in the calculations is indicated on each curve. $(\xi_J)_{\text{obs}}$ is obtained from reported low-energy resonance data. The arrows indicate positions of known levels in the target nucleus (Table II). The high-energy data ($E_n>1$ MeV) were calculated by Eq. (3) in the text.

ACKNOWLEDGMENTS

It is a pleasure to acknowledge the cooperation of the Los Alamos and Brookhaven Physics Departments in performing irradiations and in making their facilities available to us. In particular we are indebted to Dr. A. Schardt, Dr. K. Smith, Dr. S. Bame, Dr. J. Perry, and Dr. R. Taschek of Los Alamos; Dr. D. Alburger, Dr. N. Glasoe, and Dr. C. Baker of Brookhaven; and Miss Frances Latell of the Livermore Laboratory. We would also like to thank Dr. B. Margolis for his advice and suggestions with respect to the calculated cross sections.